Cellular and Molecular Life Sciences (2024) 81:373
https://doi.org/10.1007/s00018-024-05400-2

ORIGINAL ARTICLE

Sensory nerves drive migration of dental pulp stem cells via the CGRP-Ramp1 axis in pulp repair

Chunmeng Wang[1] · Xiaochen Liu[1] · Jiani Zhou[1] · Xiaoyi Zhang[1] · Zihao Zhou[1] · Qi Zhang[1]

Received: 1 September 2023 / Revised: 17 July 2024 / Accepted: 6 August 2024

Abstract

Dental pulp stem cells (DPSCs) are responsible for maintaining pulp structure and function after pulp injury. DPSCs migrate directionally to the injury site before differentiating into odontoblast-like cells, which is a prerequisite and a determinant in pulp repair. Increasing evidence suggests that sensory neuron-stem cell crosstalk is critical for maintaining normal physiological functions, and sensory nerves influence stem cells mainly by neuropeptides. However, the role of sensory nerves on DPSC behaviors after pulp injury is largely unexplored. Here, we find that sensory nerves released significant amounts of calcitonin gene-related peptide (CGRP) near the injury site, acting directly on DPSCs via receptor activity modifying protein 1 (RAMP1) to promote collective migration of DPSCs to the injury site, and ultimately promoting pulp repair. Specifically, sensory denervation leads to poor pulp repair and ectopic mineralization, in parallel with that DPSCs failed to be recruited to the injury site. Furthermore, in vitro evidence shows that sensory nerve-deficient microenvironment suppressed DPSC migration prominently among all related behaviors. Mechanistically, the CGRP-Ramp1 axis between sensory neurons and DPSCs was screened by single-cell RNA-seq analysis and immunohistochemical studies confirmed that the expression of CGRP rather than Ramp1 increases substantially near the damaged site. We further demonstrated that CGRP released by sensory nerves binds the receptor Ramp1 on DPSCs to facilitate cell collective migration by an indirect co-culture system using conditioned medium from trigeminal neurons, CGRP recombinant protein and antagonists BIBN4096. The treatment with exogenous CGRP promoted the recruitment of DPSCs, and ultimately enhanced the quality of pulp repair. Targeting the sensory nerve could therefore provide a new strategy for stem cell-based pulp repair and regeneration.

Keywords Sensory nerve · Wound healing · Mesenchymal stem cells · Cell communication · Neuropeptides

Introduction

Dental pulp diseases are highly prevalent worldwide and result in substantial healthcare burdens [1]. Timely repair is crucial for the effective restoration of function and preservation of pulp vitality. Dental pulp stem cells (DPSCs) play a pivotal role in responding to pulp injury by migrating towards the injury site first and then differentiating into odontoblast-like cells, which synthesize reparative dentin, immediately below the site of damage to preserve pulp vitality [2, 3]. The migration of DPSCs is considered a prerequisite and a determinant for therapeutic efficacy, although multiple behaviors of DPSCs contribute to pulp repair [4]. The favorable repair could be completed by recruiting more endogenous DPSCs to the injury sites [5, 6]. However, there is an unmet need for an improved understanding of factors associated with DPSC migration.

The migration of DPSCs is subject to diverse signals emanating from the extracellular microenvironment [7, 8]. A complex network of nerves in the dental pulp embraces DPSCs intimately, shaping a nerve-derived microenvironment [9–11]. Nerves account for 40% of the pulp volume, primarily sensory nerve fibers originating from the trigeminal ganglion [12, 13]. However, the role of sensory nerves in DPSC migration is unclear, especially in the directional migration of DPSCs after pulp injury. Recent studies have

✉ Qi Zhang
qizhang@tongji.edu.cn

[1] Department of Endodontics, Stomatological Hospital and Dental School of Tongji University, Shanghai Engineering Research Center of Tooth Restoration and Regeneration, No.399 Yanchang Middle Road, Jing'an District, Shanghai 200072, China

Published online: 28 August 2024

identified sensory neural signals as a critical mediator of stem cell dynamics. Gao et al. found that sensory nerves influence hematopoietic stem cells directly, independent of sympathetic nerves, facilitating their mobilization from the bone marrow to the whole body and enhancing the efficacy of hematopoietic stem cell transplantation [14]. While several studies have shown that sensory denervation influences the differentiation or self-renewal capacity of mesenchymal stem cells (MSCs), it is unclear whether sensory nerves impact MSC migration [15, 16]. Therefore, the role of pulpal sensory nerves in regulating the behaviors of DPSCs after pulp injury deserves to be explored, especially migration.

Local injury signals trigger MSC migration mainly through chemotaxis [17, 18]. Chemokine receptors on MSCs recognize elevated levels of soluble molecules at the injury site, inducing the directional migration towards an external gradient of diffusible chemoattractant [19]. Upon injury signals, sensory nerves secrete various neuropeptides as intercellular messenger molecules [20]. Several studies have suggested that the migration of MSCs can be regulated by sensory nerve neuropeptides, such as calcitonin gene-related peptide (CGRP), substance P (SP), and neuropeptide Y (NPY), interacting with their corresponding receptors [21, 22]. The exogenous administration of CGRP enhances the recruitment of bone marrow mesenchymal stem cells (BMSCs) to injury sites, promoting the healing of the mandible [23]. In vitro investigations have revealed that the binding of substance P (SP) to its receptor NK1R can stimulate the migration of BMSCs [24]. Furthermore, neuropeptide Y (NPY) has been implicated in regulating postmyocardial infarction remodeling by promoting MSC migration [25]. Notably, CGRP and SP expression levels are observed to increase in proximity to the site of pulp injury [26, 27]. It is unclear whether sensory nerves regulate the migration of DPSCs through the release of neuropeptides as well as the specific neuropeptides predominantly involved, although in vitro studies have shown that neuropeptides affect the proliferation, differentiation, and apoptosis of DPSCs [27, 28].

In this study, we explored the role of sensory nerves on DPSC behaviors after pulp injury and demonstrated the most pronounced effect on migration. Our findings revealed that the neuropeptide CGRP, released by sensory nerves originating from the trigeminal ganglion, directly acts DPSCs through Ramp1, facilitating collective migration towards the injury site and ultimately promoting pulp repair. Taken together, these results highlight the role of sensory nerves in regulating the collective migration of DPSCs after pulp injury and may offer novel approaches for promoting pulp repair and regeneration. This study in dental pulp also provides a valuable model for investigating the crosstalk between sensory nerves and MSCs.

Materials and methods

Human dental pulp tissue samples

The dental pulp tissues utilized in this study were procured as discarded third molar teeth, which were obtained after surgical extraction from a healthy adolescent donor with prior approval from the Affiliated Stomatology Hospital of Tongji University, in accordance with the Ethics Review Board (2021-SR-09). The patients who participated in this study provided written informed consent and were diagnosed based on published guidelines. Furthermore, patients who received antibiotics or anti-inflammatory drugs were excluded from the study.

Experimental animals

All animal experiments were approved by the Ethics Review Board of the Affiliated Stomatology Hospital of Tongji University (2021-DW-21). Male Sprague–Dawley rats aged 6 to 8 w (weighing 200 to 250 g, purchased from SPF (Beijing) Biotechnology Co., Ltd) housed in a controlled environment with 12-hour day/night cycles with optimal temperature and fed with a standard laboratory diet and allowed ad libitum access to drinking water. A total of 175 male rats were randomly assigned according to the study protocols. All experimental procedures followed the ARRIVE guidelines 2.0. Animals were randomized into different groups, and at least 4 rats were used for each group unless otherwise stated.

Inferior alveolar nerve transection (IANX)

The IANX procedure was executed in accordance with prior descriptions [29–31]. The masseter muscle was fully exposed via an extraoral horizontal incision while under general anesthesia utilizing 1% Pelltobarbitalum Natricum (Sangon Biotech, China). The mandibular bone surface was exposed through blunt dissection of the masseter muscle. A small dental round bur was employed to excise the cortex bone and reveal the IAN, followed by removing a 5 mm segment of the IAN. The muscle and skin were subsequently closed and sutured. In the control group, a sham operation was conducted, which entailed skin incision, muscle debridement, and bone shaving without severing the IAN, followed by suturing of the incised muscle and skin. On weeks 1, 2, and 4 after the operation, rats were sacrificed by intracardiac perfusion with 4% paraformaldehyde (PFA) buffered at pH 7.2–7.4. Each group comprised a minimum of four animals.

Experimental pulp injury model

Experimental pulp exposures on the occlusal surface of the mandibular first molars were prepared as described [32]. Under general anesthesia, a cavity was created with a No.1/4 round steel bur in the mesial half of the occlusal surface of the mandibular first molar. The exposed pulp in both groups was irrigated with saline for 15 s, and then gently dried with sterile paper points. Then pulps were sealed with Iroot BP plus (Innovative Bioceramix, CA, USA) and light-cured composite resin as described before [33]. On days 1, 3, 7, and 14 after the operation, rats were sacrificed by intracardiac perfusion with 4% PFA buffered at pH 7.2–7.4. Each group consisted of at least four animals.

Isolation, culture and characterization of rat DPSCs

Primary cells with and without IANX were isolated following a published protocol [26, 33, 34]. The first molars were separated from the mandible. A scalpel was used to clean soft tissue, dissected at the root/crown interface to expose the molar pulp, and maintained in PBS buffer. Then pulp tissues were digested in collagenase type I (3 mg/ml, Sigma-Aldrich, USA) for 30 min at 37 °C. Cells were then plated evenly on 6-well plates with α-MEM supplemented with 20% fetal bovine serum (FBS) and 1% penicillin-streptomycin. Flow cytometric analysis of surface antigen expression was applied to identify cultured DPSCs.

Primary culture of trigeminal ganglion (TG) neurons

TG neurons were obtained from SD rats and cultured according to the methodology outlined in a previous publication [26, 35]. The TG tissues were dissected and placed in Hank's balanced salt solution (HBSS) at a low temperature. Subsequently, the TGs were subjected to enzymatic and mechanical cell dissociation. The suspensions were centrifuged at 1000 g for 5 min at 4 °C, washed, and seeded in a 6-well plate. These isolated TG neurons were maintained in F12 medium supplemented with 10% FBS, 2% B27 supplement, 1% penicillin-streptomycin, and 500 µM l-glutamine at 37 °C and 5% CO_2 until the preparation of conditioned media. Neurons were not passaged before experiments.

Collection of conditioned media from TG neuron culture

TG neurons were extracted from cultured Rats using a complete neuronal growth medium for three days. On the fourth day, the neurons underwent two washes and were subsequently cultured in α-MEM supplemented with 2% FBS and 1% penicillin-streptomycin. Following 24 h of culture, the supernatant was collected and subjected to centrifugation at 1000 g for 10 min to eliminate any cellular debris [36].

RNA-sequencing and data analysis

Total RNA was isolated from the rat teeth of the normal, 1d, 3d, and 7d after-injury groups using TRIzol reagent (Takara, China). 16 RNA samples (4 samples in each group, 4 groups in total) were subjected to RNA sequencing. Library construction and sequencing were provided by the Novogene Bioinformatics Institute (Beijing, China) on an Illumina HiSeq 4000 platform, and 150 bp paired-end reads were generated after clustering the index-coded samples. The differentially expressed genes were screened by the threshold of 1.5-fold change and a p-value greater than 0.05. The differential genes related to the sensory nerve with TPM > 0 were used to depict the Volcano plot. The enrichment level of the biological process of gene ontology was assessed by GSEA using the databases of GO-BP.

MicroCT scanning and analysis

Mandibular bones with teeth dissected from rats were fixed in 4% PFA for 48 h. The microCT (µCT-40, Scanco Medical, Zurich, Switzerland) was employed for tissue tomography and the resultant output was obtained in DICOM format. The image data were reconstructed and analyzed using the Mimics 13.0 software.

Hematoxylin and eosin (HE) staining

The standard HE staining protocol was followed, whereby the tissue samples were first fixed in 4% PFA at 4 °C for 48 h, followed by demineralization in a 10% EDTA solution at 4 °C for approximately 2 months with a solution change every 3 days. The samples were subsequently dehydrated using a graded ethanol series, embedded in paraffin, sectioned at 4-µm thickness, and stained with the HE staining kit (Sangon Biotech, China). The resulting stained samples were then observed using light microscopy (Zeiss, Germany).

Immunofluorescence staining and immunohistochemistry staining

Immunofluorescence staining was performed in tissues and cultured cells as previously described [35, 37, 38]. Tissues were fixed, decalcified, processed, and sectioned as described earlier. Cultured cells were fixed in 4% PFA for a duration of 15 min and subsequently washed twice with PBS. The samples were then blocked with goat serum at room temperature and incubated overnight at 4 °C with the

primary antibody as indicated. The secondary antibody, conjugated with fluorochrome, was incubated for 60 min. The actin cytoskeleton was stained using AlexaFluor 488 phalloidin (Yeasen, China, 1:1000) or rhodamine-conjugated phalloidin (Yeasen, China, 1:100), while the nuclei were counterstained with DAPI for 5 min. The sections were then mounted on glass and subjected to microscopy.

Immunohistochemistry staining. The tissues underwent fixation, decalcification, processing, and sectioning as described above. Hyaluronidase was utilized for antigen retrieval. Endogenous peroxidase activity was blocked using a 3% H_2O_2 solution and goat serum. Subsequently, the tissues were incubated with primary antibody at 4 °C overnight. Following PBS washing, biotinylated secondary antibodies were applied, and the samples were further processed using streptavidin peroxidase and a DAB Detection Kit (MXB, China) according to the manufacturer's instructions.

A complete list of antibodies is shown in Supplementary Table S1. Positively stained areas were measured with Image J. Negative and positive controls were employed in all immunofluorescence and immunohistochemistry studies to ensure an accurate interpretation of our results.

Scanning electron microscopy (SEM)

Samples were dehydrated by ethanol gradient, fixed in 4% paraformaldehyde, then coated with a 20–30 nm thin metallic layer of gold in a sputter coating machine and witnessed under SEM. The accelerating voltage of the SEM was 20 kV whereas different magnifications (based on convenience) were utilized.

Alkaline phosphatase (ALP) activity assay and alizarin red S staining

The present study assessed odontoblastic activities through the utilization of alkaline phosphatase (ALP) and alizarin red. Rat DPSCs were cultured in 24-well plates and exposed to odontoblastic differentiation medium, which consisted of 2 mM β-glycerophosphate (Sigma-Aldrich, USA), 50 mg/mL ascorbic acid (Sigma-Aldrich, USA), and 100nM dexamethasone (Sigma-Aldrich, USA). The medium was refreshed every 2 days, and after 7 days, cells were fixed with 4% PFA and stained for ALP using an ALP staining kit (Beyotime, China). Following a 21-day incubation period, cells were treated with 4% PFA and subsequently stained with 0.2% alizarin red (Sigma-Aldrich, USA) for 20 min at ambient temperature. The positive area was observed under a stereoscopic microscope (Zeiss, Germany).

Cell proliferation assay

Cell proliferation was quantified using CCK8 assays. DPSCs subjected to varying conditions were allocated into 96-well plates, with each well containing 3000 cells, and were subsequently incubated under identical conditions. CCK8 solution was introduced into the wells and incubated for 1 h. The absorbance of proliferation at 450 nm was determined using a microplate reader (Bio-Tek, Hercules, CA, USA). Experiments were repeated three times.

Wound healing/scratch assay

The wound healing assay was performed as previously described [39, 40]. For the wound healing assay, cells (3×10^5cells/well) were seeded into 6-well culture plates (Corning-Costar, USA). When cells reached > 90% confluence, cells were starved overnight in medium with a low concentration (2%) of FBS, then wound scratches were made by a 200 μL pipette tip Cells were incubated in medium with a low concentration (2%) of FBS and mitomycin (1.5 μg/mL, Sigma) was always added to suppress cell proliferation. After 24 h, wound closure was photographed. The experiments were performed in triplicate.

Transwell chemotaxis assay

Transwell chemotaxis assays were performed as previously described. Chemotaxis experiments were performed using a 24-well transwell chamber (12 μm pore size, Corning Incorporated, USA). 3×10^4 cells were seeded into the upper chamber, provided with serum-free medium, and permitted to pass through a polycarbonate filter. The upper chamber was then incubated in a 24-well plate chamber. Chemoattractant was added to the lower chamber. A cotton swab was used to remove cells from the upper chamber, the migrated cells on the lower surface of the chamber were fixed with 4% PFA and stained with 0.1% crystal violet. Migrated cells were photographed with an inverted microscope.

Re-analysis of scRNA-seq data

The scRNA-seq data utilized in this study were sourced from the GEO database (GSE197289, GSE164157) and analyzed using Cell Ranger (version 3.1.0) software. The resulting clusters were visualized through t-distributed Stochastic Neighbor Embedding (tSNE). Normalization, dimensionality reduction, and clustering were conducted for each of the major cell types, followed by cluster annotation based on the average expression of curated gene sets specific to the respective cell types. To explore potential interactions between various cell types, an analysis of cell-cell

communication was conducted through the utilization of CellPhoneDB. This resource serves as a publicly accessible database of meticulously curated receptors and ligands, along with their respective interactions. The analysis of CellPhoneDB was executed through the implementation of the Python package (1.1.0).

Real-time quantitative PCR

Total RNA was extracted using Trizol (Takara, China), using a cDNA Synthesis SuperMix for quantitative polymerase chain reaction (qPCR) with gDNA Eraser (Yeasen, China). To quantify mRNA levels, real-time qPCR was performed using a qPCR SYBR Green Master Mix (Yeasen, China) on a LightCycler®96 (Roche, Switzerland) device. Data were normalized to the housekeeping gene *β-actin*, and relative expression was evaluated using the $2^{-\Delta\Delta Ct}$ method. Primers were designed using Primer 6 software, and the primer sequences are listed in Supplementary Table S2.

Direct pulp capping with medicaments

Direct pulp capping with different medicaments was prepared as previously described Under general anesthesia [41]. A cavity was created with a No.1/4 round steel bur in the mesial half of the occlusal surface of the mandibular first molar. The exposed pulp was gently washed with saline. Next, a gelatin sponge (Spongel; Astellas Pharma) containing 100 nM CGRP (HY-P0203A, MCE, USA)) or BIBN4096(HY-10095, MCE, USA)or PBS alone as control was gently covered on the exposure site. Pulps were sealed with Iroot BP plus (Innovative Bioceramix, CA, USA) and light-cured composite resin. Rats were sacrificed on days 3 and 14 after surgery. Each group consisted of at least four animals.

Statistical analysis

All data are presented as mean ± SEM ($^{*}P < 0.05$; $^{**}P < 0.01$; $^{***}P < 0.001$). Student t-test was used for comparisons between 2 groups and the ANOVA test was to assess more than 2 groups. Analyses were performed with GraphPad Prism v9.0.0 (GraphPad Software).

Results

Denervation of sensory nerves leads to poor pulp repair and ectopic mineralization

Human dental pulp nerves primarily consist of sensory nerves, with a minor presence of sympathetic nerves [13]. We examined the distribution of the sensory nerve marker TRPV1 and the sympathetic nerve marker TH within the overall nerve density of rat molar pulp (Fig. S1a). Our observations revealed that sensory nerve fibers constitute the overwhelmingly predominant constituent of rat molar pulp nerves. Furthermore, pulpal nerves form substantial bundles within the root canal pulp, which subsequently divide into intricate, compact nerve fibers upon reaching the crown pulp cavity, rendering the pulp more sensitive to external stimuli (Fig. S1b).

We conducted RNA-seq analysis of normal and injured pulp tissue, and GO enrichment analysis showed distinct neurogenesis and neurotransmitter biosynthetic processes (Fig. S2 a, b). Following the method previously described [42], DEGs related to various facets of sensory nerves are altered to varying degrees after pulp injury (Fig. S2 c, d), conforming to previous findings [43, 44]. The staining of β3-tubulin (a cytoskeletal protein often used as a pan-neural marker) revealed a significant increase in pulp nerve density after pulp injury, and the highest density was observed on day 3 (Fig. S2e). This observation aligns with the established notion that neurogenesis reaches its zenith at early injury in bone [45]. We speculated that sensory nerves may be involved in the pulp healing process.

To ascertain whether sensory nerves impact repair after pulp injury, we established a pulp injury model in rats 2 weeks after inferior alveolar nerve dissection (Fig. 1a). Inferior alveolar nerve transection (IANX) was performed successfully (Fig. S3a), and the uninjured pulp did not exhibit any significant changes within 4 w after sensory nerve removal (Fig. S3b). Except for the higher incidence of calcified clusters, we did not observe significant differences in histology between the two groups at 3d postinjury (Fig. 1b-d). However, microCT analysis and HE staining revealed that rats in the sham group formed restorative dentin at the site of pulp injury after 7 and 14 d. In contrast, rats in the IANX group did not form a complete restorative dentin bridge but instead exhibited scattered ectopic mineralization within the pulp chamber, the number of calcified clusters and the area of calcification were larger than those in the sham group (Fig. 1e-g, Fig. S4a-c). Scanning electron microscopy of the mineralized tissues formed in both groups at 14 d postinjury demonstrated that the restorative dentin formed in the sham group exhibited uniform structure and orientation, while calcified masses formed in the IANX group displayed chaotic structure and disordered orientation (Fig. 1h). Additionally, the results of immunohistochemical staining revealed a significant increase in the expression of DSPP and DMP1 among the two groups, which was related to odontogenic differentiation. However, the location of the positive expression was close to the injury site in the sham groups but was diffusely distributed in the IANX groups,

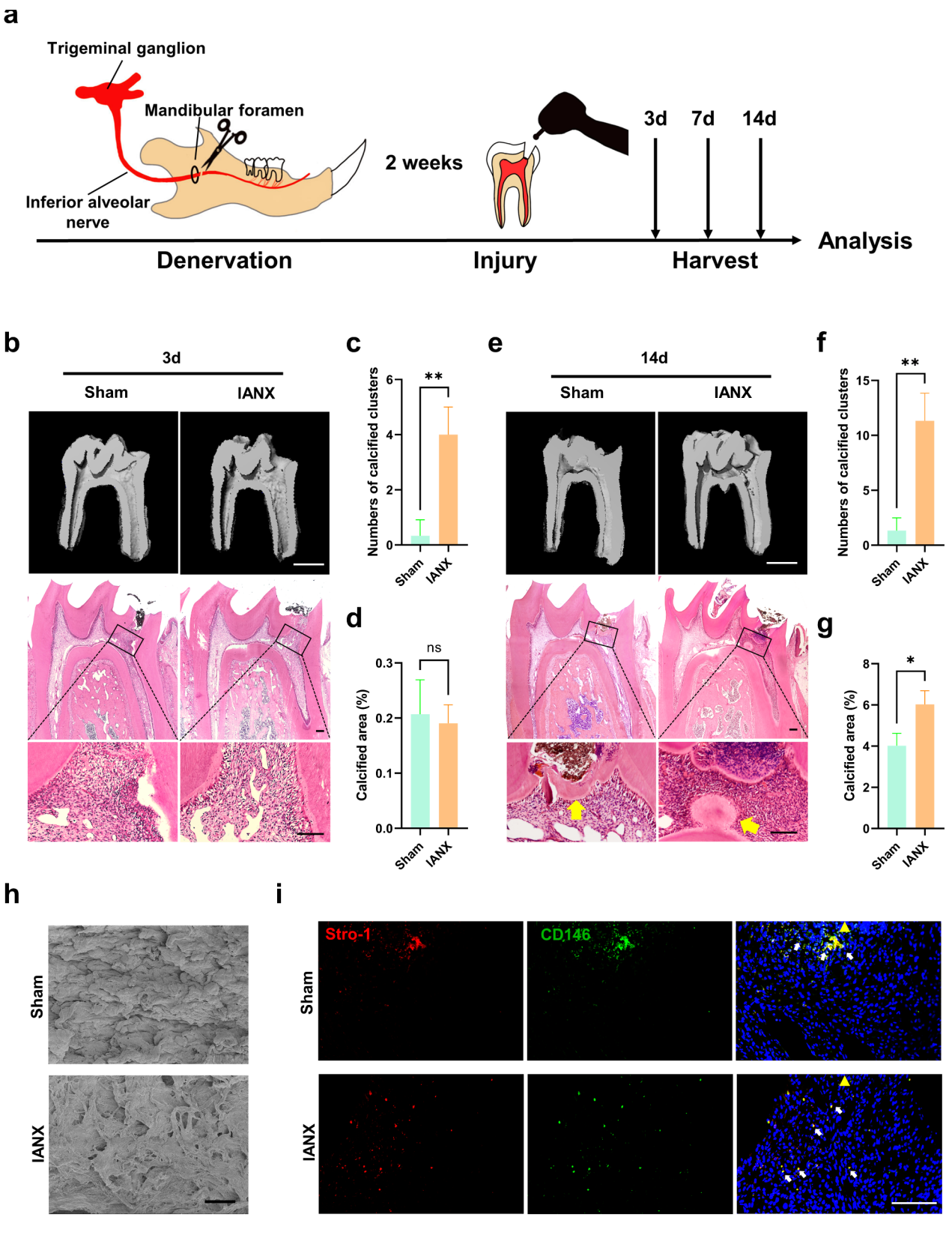
a
Trigeminal ganglion
Mandibular foramen
Inferior alveolar nerve
2 weeks
3d
7d
14d
Denervation
Injury
Harvest
Analysis
b
3d
Sham
IANX
c
Numbers of calcified clusters
**
Sham
IANX
d
Calcified area (%)
ns
e
14d
f
g
*
h
i
Stro-1
CD146

Fig. 1 Denervation of sensory nerves leads to poor pulp repair and ectopic mineralization. **a** Schematic illustrating the denervation and pulp injury strategy ($n=4$). **b** MicroCT and HE staining of the Sham and IANX groups at 3 d. MicroCT scale bar = 1 mm; HE scale bar = 100 μm. **c** Quantification of the calcified clusters number of MicroCT in **b** (**$P<0.01$, $n=3$). **d** The percentage of the calcified area of the total pulp area (%) of MicroCT in **b** (ns indicates $P\geq0.05$, $n=3$). **e** MicroCT and HE staining of the Sham and IANX groups at 14 d. Yellow arrows indicate mineralized tissue. MicroCT scale bar = 1 mm; HE scale bar = 100 μm. **f** Quantification of the calcified clusters number of MicroCT in **e** (**$P<0.01$, $n=3$). **g** The percentage of the calcified area of the total pulp area (%) of MicroCT in **e** (ns indicates $P\geq0.05$, $n=3$). **h** Scanning electron microscopy of restorative dentin bridges in the Sham group and mineralized masses in the IANX group at 14 days after pulp injury as indicated by yellow arrows in **c**. Scale bar = 20 μm. **i** Immunofluorescence staining of Stro-1(red) and CD146 (green) in the pulp close to the injury of the Sham and IANX groups at 3 d. Images are at a similar magnification with the lower panel of **b**. White arrows indicate co-staining. Yellow arrows indicate dental pulp injury sites. Scale bar = 100 μm

and DSPP and DMP1 positive area were larger in the IANX group (Fig. S4d, f). Besides, we performed PCNA staining to detect cell proliferation. PCNA-positive cells were located mainly below the site of injury in the sham group and elsewhere in the coronal pulp away from this site in the IANX group. Still, they agree with each other quantitatively (Fig. S4e, g).

Denervation of sensory nerves did not impair mineralization formation, but mineralization was not in a desirable position. Moreover, we marked DPSCs using CD146 and Stro-1 [46], our findings indicate a close relationship between the spatial distribution of nerve fibers and the localization of DPSCs either in rat or human injured pulp (Fig. S5). Consequently, we speculated that poor pulp repair and ectopic mineralization may be attributed to the distribution of DPSCs after injury. Immunofluorescence staining revealed that DPSCs were observed to gather near the injury site in the sham group. Conversely, in the IANX group, the distribution of DPSCs was distant from the injury site (Fig. 1i).

Additionally, previous studies on a mouse incisor model showed the detrimental effect of the transected inferior mandibular nerve on the cellular composition in the apical region of a continuously growing incisor [30]. It is unclear whether the poor repair is due to a lack of progenitor and stem cells in the pulp of rat molars after IANX. Consequently, to determine whether stem cell numbers are reduced in the nerve-deficient environment in rat molars, we tested the transcription of stem cell marker genes in uninjured dental pulp tissue in the sham groups and IANX groups by real-time qPCR following the approach in previous literature [47, 48]. Moreover, we examined the total number of cells and the percentage of Stro-1 and CD146-positive cells in the pulp following the methods outlined by Hayano et al. [30]. The findings indicated that there was no significant statistical difference between the two groups (Fig. S6). These findings suggest that sensory nerves may influence the biological behavior rather than the number of DPSCs following pulp injury.

The sensory nerve-deficient microenvironment reduces the migration ability of DPSCs

To further determine the impact of sensory nerves on the behavior of DPSCs in pulp injury, DPSCs were isolated from the first mandibular molars of rats subjected to IANX, with a sham group serving as a control. Flow cytometry characterized the surface antigens of the two groups of DPSCs (Fig. S7a, b). To simulate an inflammatory injury model, the cells were treated with LPS for 24 h, as in previous studies (Fig. 2a) [33, 49].

We next examined behaviors of DPSCs related to repair after IANX, including cell proliferation, migration and differentiation. The CCK8 assay was used to evaluate the cell proliferation of each group in vitro (Fig. 2b). The proliferation rate of the IANX groups slowed, but exponential cell growth continued. The LPS injury group did not show any noticeable differences, and no significant difference was observed on day 5, which coincided with the immunohistochemical staining results. These data suggest that differences in cellular proliferation are not the leading cause of poor pulp repair and ectopic mineralization. Subsequently, alkaline phosphatase (ALP) staining and mineralized nodule staining (Alizarin red) were conducted at 7 and 14 days after culture, respectively (Fig. 2c-f). Consistent with the in vivo immunohistochemical staining, the IANX group exhibited enhanced odontoblastic differentiation and production of mineralized extracellular matrix. These data exclude that poor pulp repair may be due to the abnormal differentiation ability of the DPSCs in the microenvironment of sensory nerve deficiency.

To evaluate the migratory capacity of different groups of DPSCs, we performed scratch and transwell experiments, and the IANX group had a reduced wound healing rate and a reduced number of cells crossing the transwell, demonstrating an impaired migration ability in the IANX group. LPS treatment promoted migration in both groups, and injury activates cell migration capability (Fig. 2g, i, j). Moreover, pictures were taken of the same live cells in 12 h. Cells in the Sham group changed morphology, polarized, and moved more frequently. Cells in the IANX group were round to oval or polygonal, and the shape changed little, with the relative position does not vary appreciably over time (Fig. S8).

Since cell morphology is closely associated with cell migration, we examined more than one morphological indication in each group. The cytoskeleton coordinates cellular morphology and migration, and cytoskeletal changes

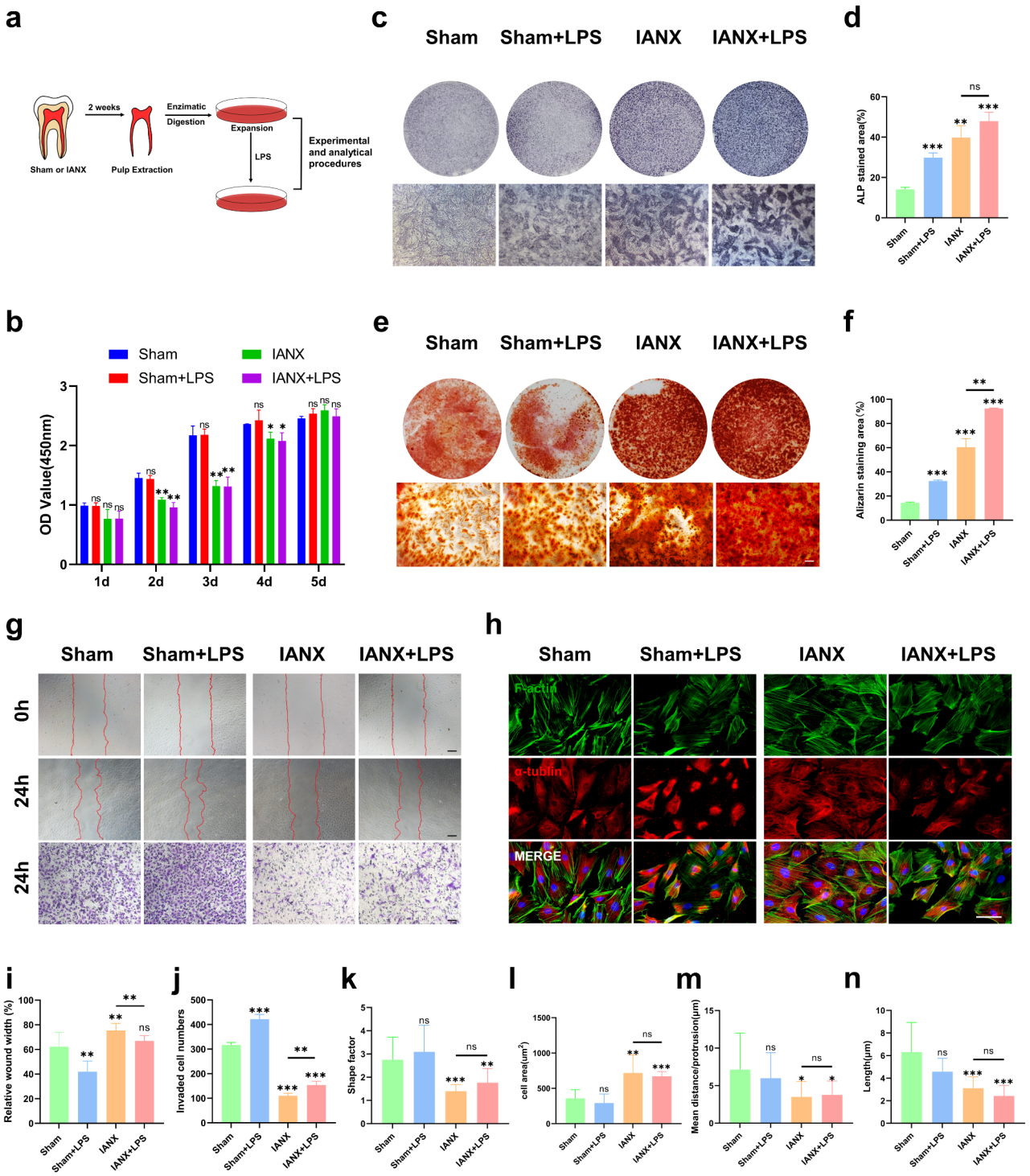

were assessed by immunofluorescence staining for F-actin and α-tubulin (Fig. 2h). The IANX group exhibited significant changes in morphology. Specifically, DPSCs in the IANX group were rounder in shape rather than long and shuttle-shaped (Fig. 2h). The quantification of differences in morphology can be performed using the shape factor and cell area. The statistical analysis indicated that the IANX group tended to have a rounded shape, decreased morphological cell polarity, and an enlarged cell area in comparison to the Sham group (Fig. 2k, l). Additionally, the protrusions

Fig. 2 The sensory nerve-deficient microenvironment influences the behaviors of DPSCs. **a** Primary culture of dental pulp stem cells (DPSCs) from rat mandibular first molars. DPSCs were subsequently stimulated with LPS (1 μg/ml). **b** Cell proliferation was detected by CCK8 assay, OD values are shown as the mean ± SEM (**$P<0.01$, *$P<0.05$, ns, not significant, $P>0.05$). **c** Alkaline phosphatase activity staining of DPSCs with different treatments. Scale bar = 100 μm. **d** Quantitative analysis of ALP activity (ALP positive area/total area) is presented in **c** (ns indicates $P\geq0.05$, **$P<0.01$, ***$P<0.001$, $n=3$). **e** Alizarin red staining of DPSCs with different treatments. Scale bar = 100 μm. **f** Quantitative analysis of alizarin red staining was presented in **e** (**$P<0.01$, ***$P<0.001$, $n=3$). **g** Representative images of wound healing and Transwell migration assays. Scale bar = 100 μm. **h** Cytoskeletal changes were assessed by immunofluorescence staining for F-actin (phalloidin, green) and α-tubulin (red). Scale bar = 100 μm. **i** Quantified results of wound healing assay in **g** (ns indicates $P\geq0.05$, **$P<0.01$, $n=3$). **J** Quantified results of Transwell assay in **g** (**$P<0.01$, ***$P<0.001$, $n=3$). **k** Shape factor is the ratio of the major to the minor axis (ns indicates $P\geq0.05$, **$P<0.01$, ***$P<0.001$, $n=15$). **l** Cell area is the area of a cross-section of the cell soma (ns indicates $P\geq0.05$, **$P<0.01$, ***$P<0.001$, $n=15$). **m** Summary graph showing protrusion density (mean distance between protrusions) (ns indicates $P\geq0.05$, *$P<0.05$, $n=15$). **n** Protrusion length. (ns indicates $P\geq0.05$, ***$P<0.001$, $n=15$)

density and length of DPSCs are related to migration, our results showed that the distance between protrusions was reduced with an increased frequency in the IANX group, while the length of the protrusions was shorter (Fig. 2m, n). The higher density limited the length of the extending protrusions, thus restricting cell migratory ability. Notably, no significant difference was observed between the LPS injury group and the non-LPS group. It suggests that the migration capacity of DPSCs is still reduced in the IANX group after pulp injury.

Overall, we were able to establish that sensory nerves facilitate DPSC migration following pulp injury; however, the precise mechanism and mediators involved remain unclear.

Sensory nerves regulate DPSCs directly through the CGRP-Ramp1 axis

We integrated and reanalyzed single-cell (sc) RNA-seq data from the human trigeminal ganglion (GSE197289) and human dental pulp (GSE164157). We identified neurons, DPSCs, and other cell types in the pulp from crude clusters based on the expression of typical marker genes (Fig. S9a-f). Subsequently, we employed CellphoneDB to explore the cell-cell interaction network among the identified cell types, which revealed a close association between neurons and DPSCs. We identified 257 receptor-ligand pairs between two cell types (Fig. S9g). However, our hypothesis suggests that neuropeptides released by sensory nerves originating from the trigeminal ganglion may directly facilitate the migration of DPSCs. The heatmap illustrates the high expression of neuropeptides in the trigeminal ganglion according to previous research [50], as well as the presence of corresponding neuropeptide receptors on DPSCs [51], indicating that the CGRP-Ramp1 axis is the most potent signaling axis between the two (Fig. 3a). Ramp1 is required for high-affinity binding of CGRP, which forms a receptor complex with its coreceptor calcitonin-receptor-like receptor (Calcrl) to bind CGRP. Therefore, we focused on the CGRP-Ramp1 axis in the following study, and utilized BIBN4096 (also known as olcegepant), an antagonist of Ramp1 signaling as reported previously [52].

To investigate the role of the CGRP-Ramp1 axis, we collected injured molars and ipsilateral trigeminal ganglia at 1, 3, and 7 d post-injury. The results of qPCR analysis revealed that the gene expression of *calca* in the trigeminal ganglion was highest at 1 d postinjury (Fig. S10a). Immunohistochemical analysis showed that the expression levels of CGRP were most pronounced in the mandibular region (V3) of trigeminal ganglion and dental pulp at 3 d post-injury in the Sham group, while the IANX group showed negligible CGRP expression at the sites of pulp injury (Fig. 3b-e, S10b, c). The injury signal stimulated sensory nerve endings from the trigeminal ganglion to release a significant amount of CGRP at the injury site.

However, there were no statistically significant differences in Ramp1 expression across various conditions in DPSCs in vitro and in vivo (Fig. 3f-i). These findings suggested that alterations in DPSC behavior are attributed to elevation in CGRP levels rather than changes in Ramp1 expression.

Sensory nerves induce the migration of DPSCs through the CGRP-Ramp1 axis

We cultured primary trigeminal neurons from rats and collected conditioned media to measure DPSCs migration ability (Fig. 4a). Subsequently, we assessed the impact of each treatment on cell mobility via wound healing assays, and the chemotactic response to CGRP was evaluated using transwell assays (Fig. 4b).

We employed trigeminal ganglion conditioned medium (TG-CM), calcitonin gene-related peptide recombinant protein (CGRP), BIBN4096 (a CGRP receptor antagonist), and TG-CM plus BIBN4096 to treat DPSCs in different groups. Our findings indicate that both TG-CM and CGRP facilitated DPSC migration in the sham and IANX groups; however, this effect was abolished upon cotreatment with BIBN4096, while BIBN4096 alone did not significantly impact migration (Fig. 4c-h). In Transwell chemotaxis assays, TG-CM, CGRP, BIBN4096, and TG-CM + BIBN4096 were placed in the lower transwell chamber. We confirmed that both TG-CM and CGRP have chemotactic properties for DPSCs, this phenomenon could be blocked by BIBN4096.

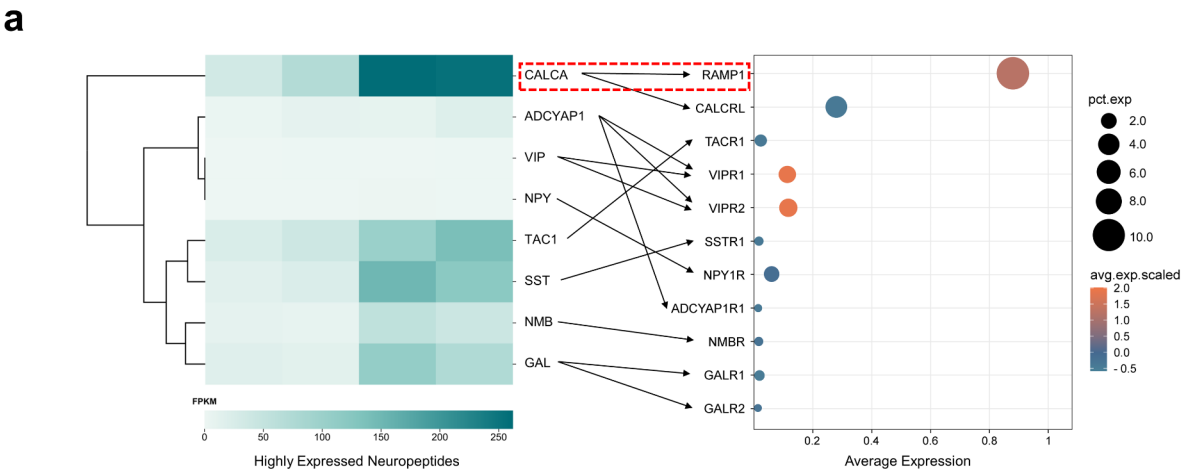
a
CALCA
ADCYAP1
VIP
NPY
TAC1
SST
NMB
GAL
RAMP1
CALCRL
TACR1
VIPR1
VIPR2
SSTR1
NPY1R
ADCYAP1R1
NMBR
GALR1
GALR2
FPKM
0 50 100 150 200 250
Highly Expressed Neuropeptides
0.2 0.4 0.6 0.8 1
Average Expression
pct.exp
2.0 4.0 6.0 8.0 10.0
avg.exp.scaled
2.0 1.5 1.0 0.5 0.0 - 0.5

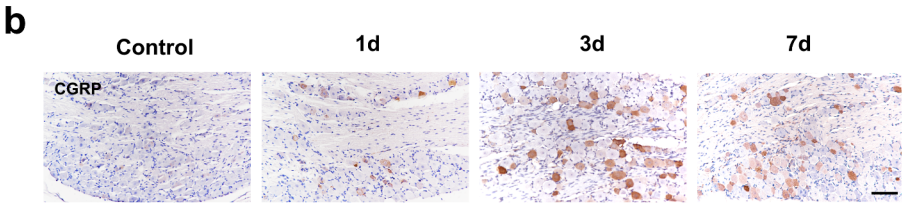
b
Control
1d
3d
7d
CGRP

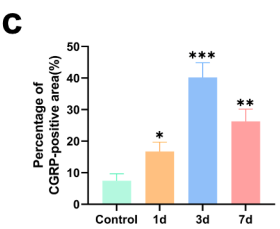
c
Percentage of CGRP-positive area(%)
Control 1d 3d 7d
* *** **

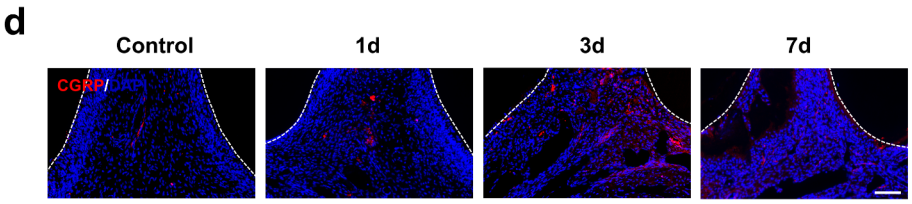
d
Control
1d
3d
7d
CGRP/DAPI

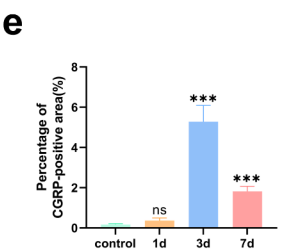
e
Percentage of CGRP-positive area(%)
control 1d 3d 7d
ns *** ***

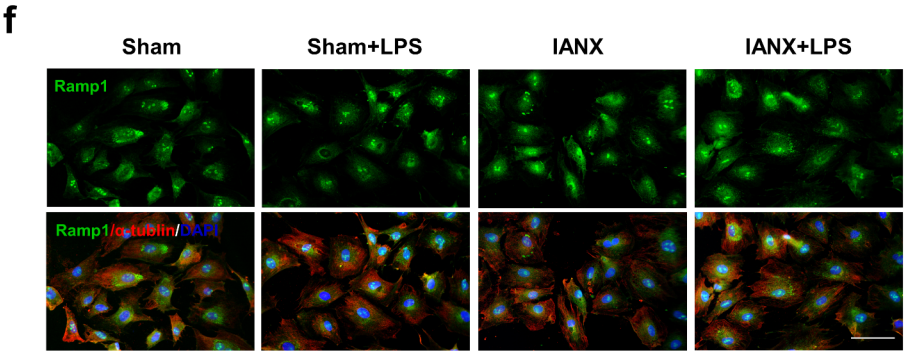
f
Sham
Sham+LPS
IANX
IANX+LPS
Ramp1
Ramp1/α-tubulin/DAPI

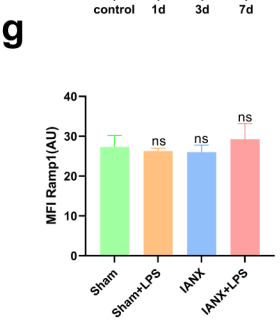
g
MFI Ramp1(AU)
Sham Sham+LPS IANX IANX+LPS
ns ns ns

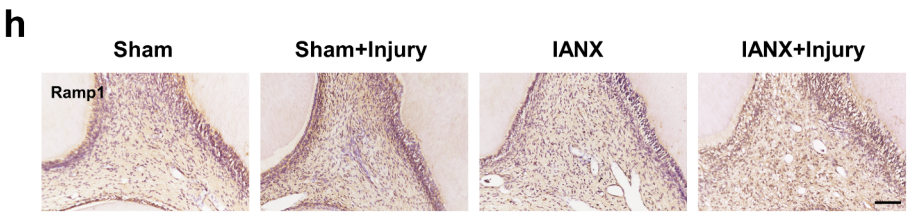
h
Sham
Sham+Injury
IANX
IANX+Injury
Ramp1

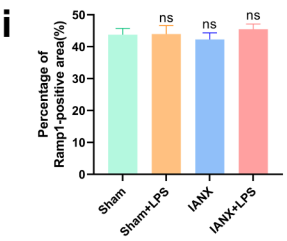
i
Percentage of Ramp1-positive area(%)
Sham Sham+LPS IANX IANX+LPS
ns ns ns

Fig. 3 Sensory nerves act directly on DPSCs through the CGRP-Ramp1 axis. **a** Left: Heatmap of the top-expressed neuropeptides in the trigeminal ganglion; Right: Dotplot of respective cognate receptor expression (denoted by arrows) in DPSCs at steady state (circle diameter reflects the percentage of cells expressing, circle color reflects relative expression abundance). **b** Immunohistochemical staining of CGRP in the trigeminal ganglion after pulp injury. Scale bar = 100 μm. **c** Statistical analysis of CGRP-positive area in the trigeminal ganglion (*$P<0.05$, **$P<0.01$, ***$P<0.001$, $n=3$). **d** Immunofluorescence imaging of CGRP in dental pulp after injury. Scale bar = 100 μm. **e** Statistical analysis of CGRP-positive area in the dental pulp (ns indicates $P\geq0.05$, ***$P<0.001$, $n=3$). **f** Immunofluorescence staining of Ramp1 (green) and α-tubulin (red) in the DPSCs of Sham and IANX groups. Scale bar = 100 μm. **g** Statistical analysis of MFI (Mean Fluorescence Intensity) in **d**. (ns indicates $P\geq0.05$, $n=15$). **h** Immunohistochemical staining of Ramp1 in the dental pulp after injury. Scale bar = 100 μm. **i** Statistical analysis of Ramp1-positive area in the dental pulp (ns indicates $P\geq0.05$, $n=3$)

Additionally, we excluded the effect of cell proliferation in migration assays with caution, and we found that CGRP did not affect the proliferation of DPSCs by CCK8 experiments (Fig. S11), which is essentially consistent with previous studies [28]. These results suggest that sensory nerves modulate DPSC migration via the release of CGRP.

Thesensory neuropeptide CGRP promotes collective cell migration by tuning intercellular junctions and cell polarity

Tissue repair relies upon collective cell migration, the movement of clustered cells as a group rather than as individual cells [53]. It requires the maintenance of multicellular polarity and intercellular junctions. The expression and distribution of CDC42 are decisive for cell polarization [54]. N-cadherin is thought to be the basis of mesenchymal intercellular junctions [55]. Hence, we conducted immunofluorescence staining of CDC42 and N-cadherin. We found that the expression of CDC42 in individual cells was more localized in the sham group but dispersed in all directions in the IANX group. There was no significant difference in the expression level between the sham and IANX groups, while LPS stimulation increased the expression of CDC42. Furthermore, following CGRP stimulation, CDC42 expression increased in all groups, with a more concentrated localization observed in the IANX group, which suggests a potential restoration of cellular polarity (Fig. 5a, b). The IANX group exhibited significantly lower levels of N-cadherin than the sham group, with no significant changes observed following LPS stimulation. However, the introduction of CGRP increased N-cadherin expression and improved intercellular junctions (Fig. 5c, d).

Collective cell migration typically adheres to a leader-follower pattern, and previous research has established p53 as a marker for leader cells [56]. Consequently, we assessed the distribution of leader cells using P53 fluorescence staining in a wound healing assay, as described by Kozyrska et al. Our findings indicate that cells located at the anterior edge of the wound in both the Sham and Sham + LPS groups displayed a statistically significant increase in p53 expression compared to cells located at the posterior edge of the wound. Conversely, P53 expression was generally heightened in the IANX and IANX + LPS groups, with no discernible leader cells during migration, both anterior and posterior to the scratch. CGRP did not significantly affect the ratio or distribution of p53-posi tive cells in the sham groups. However, in the IANX groups, CGRP reduced p53 expression levels in the posterior region of the wound, resulting in differential expression of p53 at the anterior and rear edges of the wound (Fig. 5e, f).

Therefore, CGRP was found to maintain the polarity and intercellular junctions of DPSCs and maintain a leader-follower pattern to facilitate collective cell migration of DPSCs.

Sensory nerves promote pulp healing via the CGRP-Ramp1 axis by facilitating the collective migration of DPSCs

To further investigate the potential of CGRP to enhance pulp repair through the facilitation of collective migration of DPSCs in vivo, we added CGRP and BIBN4096 during the pulp capping procedure, with PBS serving as a control vehicle in the control group. In the sham group, $CD146^+$ Stro-1^+ DPSCs were more clustered with the underside of the injury sites in both the PBS and CGRP groups, whereas with the addition of BIBN4096, DPSCs were located in a large area in the left subside of the injury (Fig. 6a). In the IANX group, the distribution of DPSCs in the PBS group was dispersed. This phenotype caused by sensory nerve deficiency was rescued by the addition of CGRP (Fig. 6b).

Following 14 d after pulp capping, the restoration of the injured pulp was observed through microCT and HE staining. In the sham group, the CGRP group exhibited more intact and dense restorative dentin bridges compared to the PBS group. Conversely, the BIBN4096 group displayed ectopic mineralization resembling that observed after inferior alveolar nerve transection (Fig. 6c, e, f). In contrast, the addition of CGRP resulted in the closure of pulp exposure in the IANX group, albeit with a small presence of mineralized masses remaining in the pulp chamber. (Fig. 6d, g, h)

The findings of this study suggest that CGRP released by sensory nerves plays a crucial role in facilitating DPSC aggregation to the site of injury, leading to good repair of pulp injury. Conversely, poor repair and ectopic mineralization occurred even in the sensory-innervated pulp after antagonists were used to block the CGRP-Ramp1 axis and thus prevent CGRP from functioning.

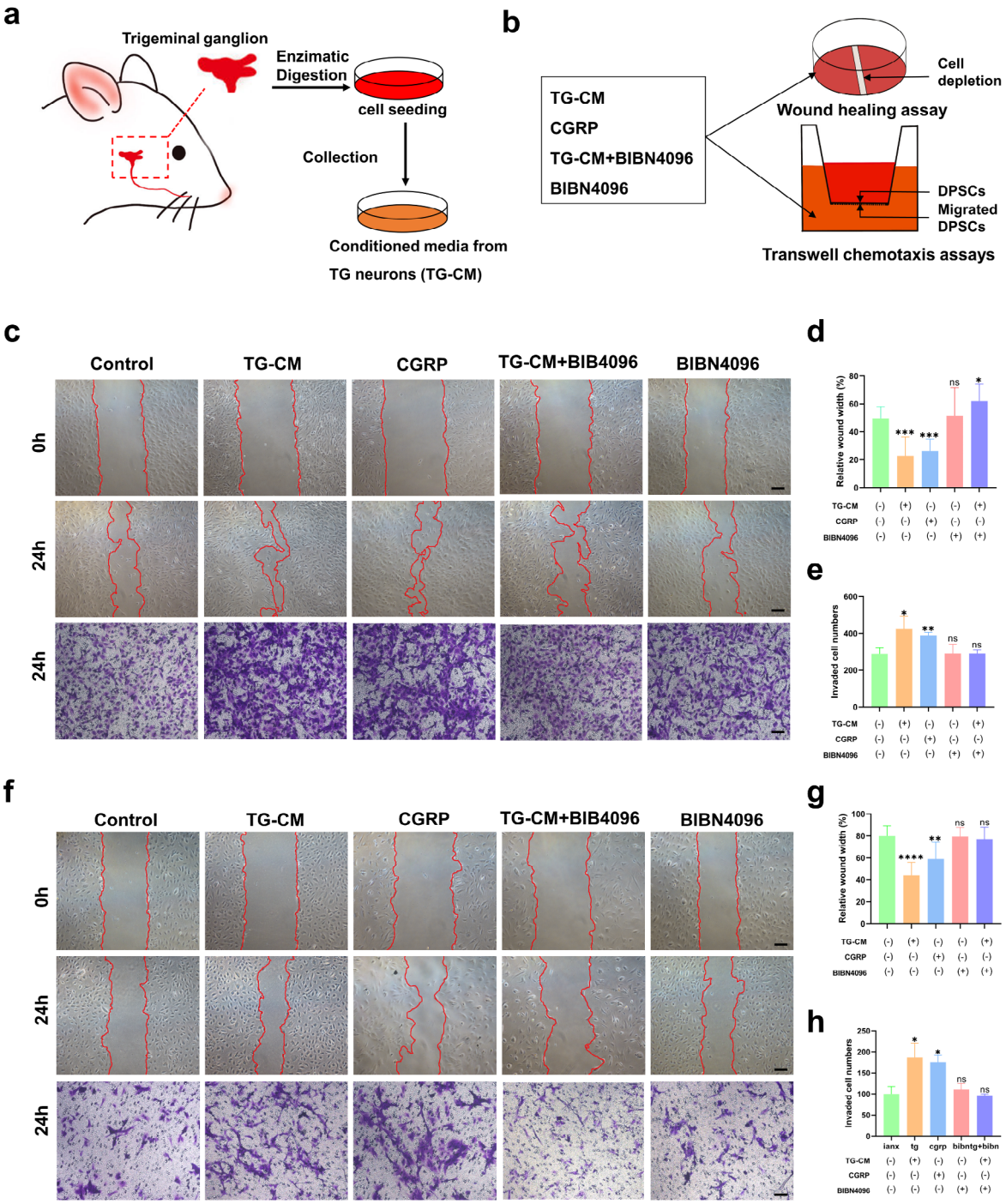

Fig. 4 The sensory nerve induces the migration of DPSCs through CGRP-Ramp1 signaling. **a**Primary culture of neurons from rat trigeminal ganglion and collection of conditioned medium.**b**Cell mobility isassessed via wound healing assays, and the chemotactic response to CGRP was evaluated using transwell assays.**c-e**Representative images and quantified results of wound healing and transwell migration assays in Sham groups stimulated with trigeminal ganglion conditioned medium (TG-CM), calcitonin gene-related peptide (CGRP, 50 ng/ml), TG-CM plus BIBN4096, and BINB4096.Scale bar = 100 μm. (*P< 0.05, **P< 0.01, ***P< 0.001, n = 3). **f-h**Representative images and quantified results of wound healing and transwell migration assays in IANX groups stimulated with trigeminal ganglion conditioned medium (TG-CM), calcitonin gene-related peptide (CGRP, 50 ng/ml), TG-CM plus BIBN4096, and BINB4096. Scale bar = 100 μm. (*P< 0.05, **P< 0.01, ***P< 0.001, n = 3)

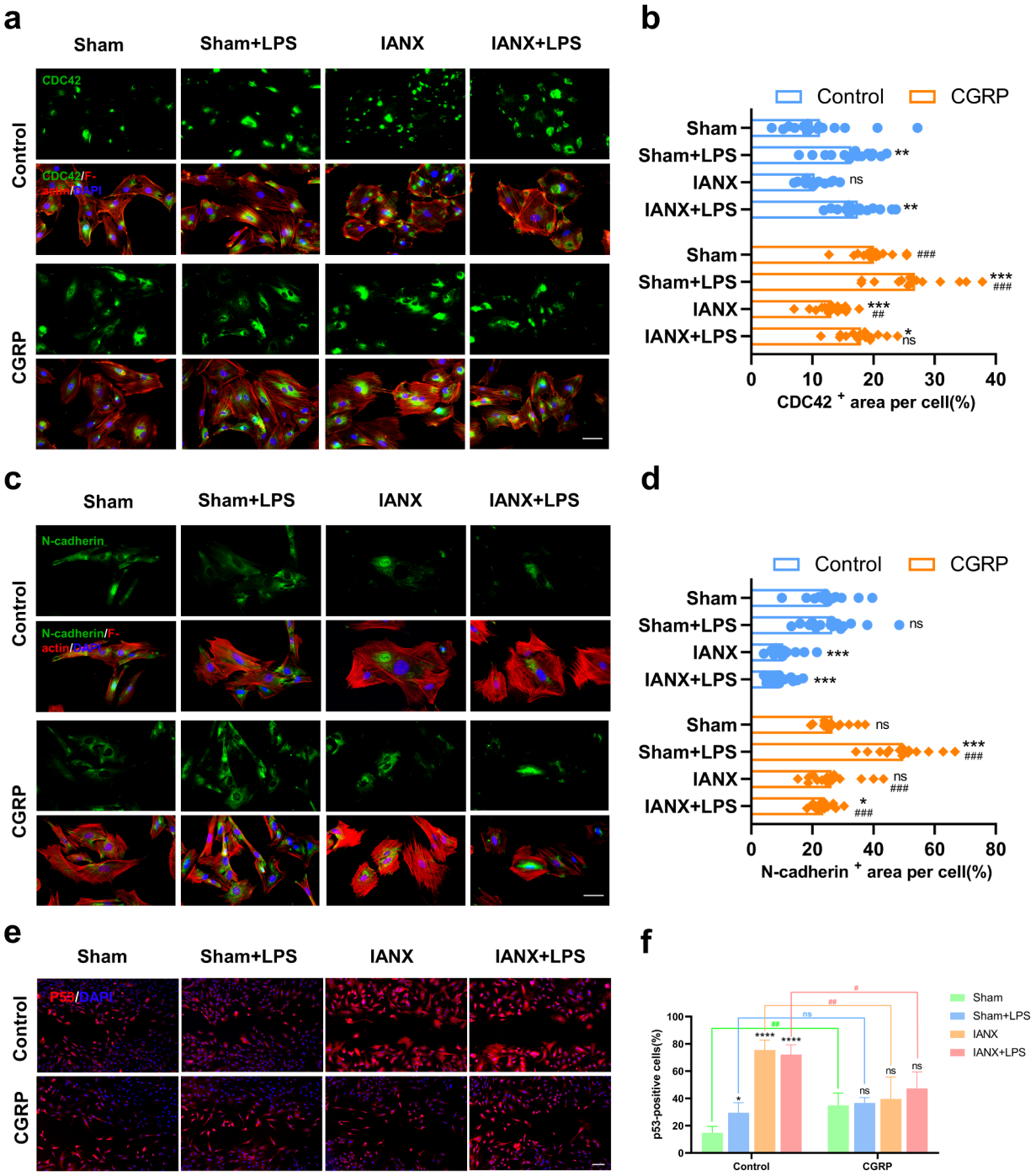

Fig. 5 The sensory neuropeptide CGRP promotes collective cell migration by tuning intercellular junctions and cell polarity. **a** Immunofluorescence staining of CDC42 (green) and F-actin (red) in the DPSCs of the Sham and IANX groups. Scale bar, 100 μm. **b** Quantified results from **a**. Asterisks (*) and pound signs (#) mark statistical differences compared with the Sham group and the same group without CGRP treatment, respectively. ($^{*/\#}P<0.05$, $^{**/\#\#}P<0.01$, $^{***/\#\#\#}P<0.001$, $n=15$). **c** Immunofluorescence staining of N-cadherin (green) and F-actin (red) in the DPSCs of the Sham and IANX groups. Scale bar, 100 μm. **d** Quantified results from **a**. Asterisks (*) and pound signs (#) mark statistical differences compared with the Sham group and the same group without CGRP treatment, respectively. ($^{*/\#}P<0.05$, $^{**/\#\#}P<0.01$, $^{***/\#\#\#}P<0.001$, $n=15$). **e** Images showing p53 staining (red) and nuclei (blue) at the wound edge of DPSCs in Sham and IANX groups. **f** Quantified results from **e**. Asterisks (*) and pound signs (#) mark statistical differences compared with the Sham group and the same group without CGRP treatment, respectively ($^{*/\#}P<0.05$, $^{**/\#\#}P<0.01$, $^{***/\#\#\#}P<0.001$, $n=15$)

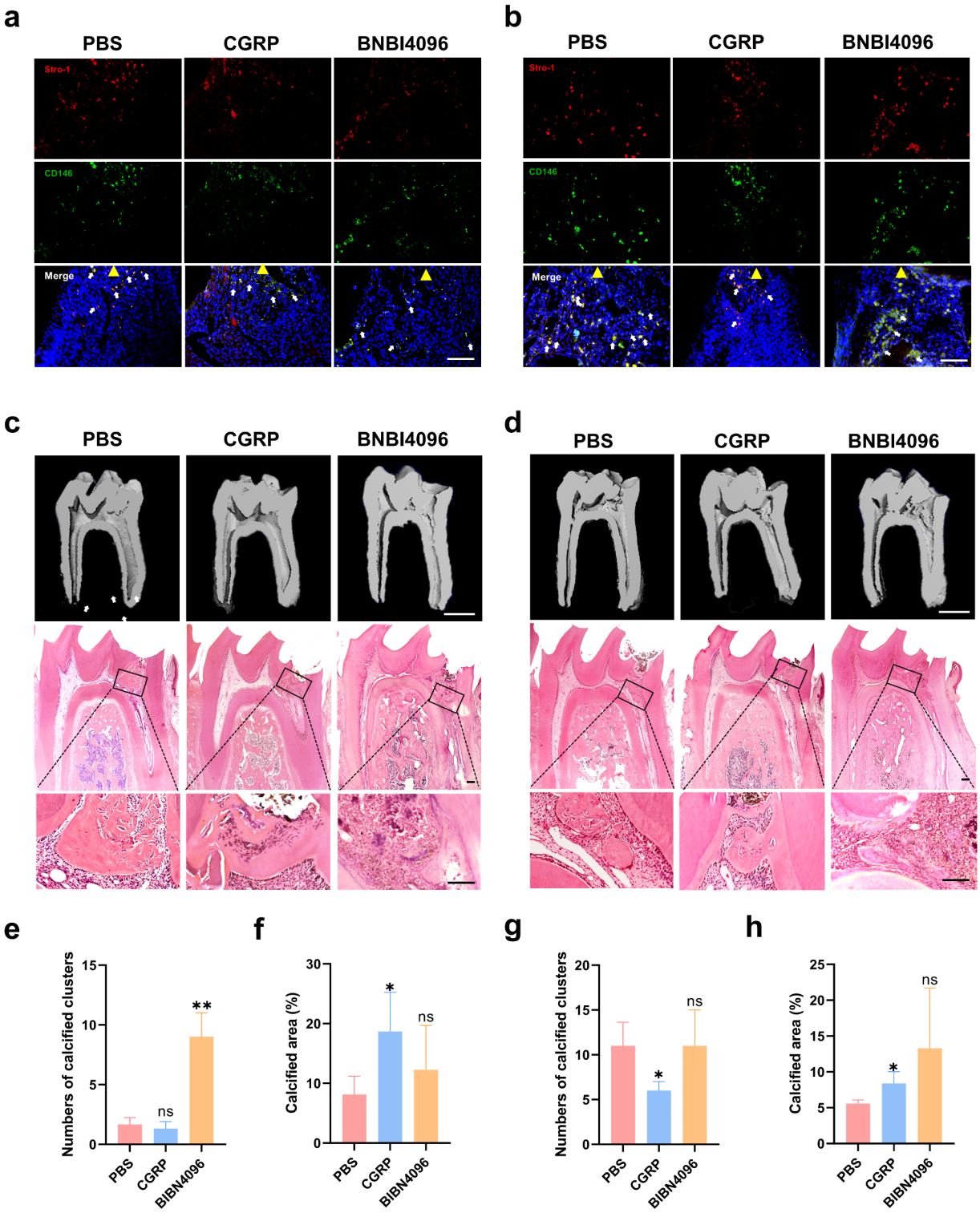

Discussion

This study is the first to demonstrate that sensory nerves promote tissue repair by facilitating the migration of mesenchymal stem cells in the pulp injury model. The sensory innervation deficits caused a reduction in the collective cell

Fig. 6 Sensory nerves promote pulp healing via the CGRP-RAMP1 axis by facilitating collective migration of DPSCs. **a** Immunofluorescence staining of Stro-1 (red) and CD146 (green) in the pulp close to the injury of the Sham group at 3 d. Yellow arrows indicate dental pulp injury sites. Scale bar = 100 μm. **b** Immunofluorescence staining of Stro-1 (red) and CD146 (green) in the pulp close to the injury of the IANX group at 3 d. Yellow arrows indicate dental pulp injury sites. Scale bar = 100 μm. **c** MicroCT analysis and HE staining of the Sham group at 14 d. Scale bar = 1 mm. **d** MicroCT analysis and HE staining of the IANX group at 14 d. MicroCT scale bar = 1 mm; HE scale bar = 100 μm. **e** Quantification of the number calcified clusters of MicroCT in **c** (**$P < 0.01$, ns indicates $P \geq 0.05$, $n = 3$). **f** The percentage of the calcified area of the total pulp area (%) of MicroCT in **c** (*$P < 0.05$, ns indicates $P \geq 0.05$, $n = 3$). **g** Quantification of the calcified clusters number of MicroCT in **d** (*$P < 0.05$, ns indicates $P \geq 0.05$, $n = 3$). **h** The percentage of the calcified area of the total pulp area (%) of MicroCT in **d** (*$P < 0.05$, ns indicates $P \geq 0.05$, $n = 3$)

migration of DPSCs, leading to substantial ectopic mineralization in the injured pulp. Although denervation may potentially induce changes in immune cells and other factors, DPSCs are mainly responsible for regulating the homeostasis, repair, and regeneration of the dental pulp. Therefore, our initial emphasis was on investigating the direct but not indirect regulatory influence of sensory nerves on DPSCs. The results of our study confirmed our hypothesis, revealing that sensory nerves from the trigeminal ganglion release CGRP, which binds receptor Ramp1 on DPSCs to promote collective cell migration after pulp injury (Fig. 7).

In our study, we constructed a model of inferior alveolar nerve dissection, distinct from models of other tissue injuries (including bones and colons), which typically use Nav1.8-, Trpv1- or TrkA-knockout mice [45, 57, 58]. Many peripheral nerves are mixed nerves and contain motor nerve fibers, but the IAN is a sensory nerve that passes through the mandibular canal, providing sensory innervation of the mandibular first molar that we used in our model [59]. Moreover, numerous studies have shown that the healing of rat molar pulp tissue is histologically comparable to that of humans [60]. It is appropriate for exploring DPSCs after molar pulp injury, similar to what is seen in a clinical setting.

In this study, we focused our attention on the effect of sensory nerves on DPSC migration. This determination was made following the careful evaluation and exclusion of alternative hypotheses, including odontogenic differentiation and proliferation of DPSCs. Previous research had predominantly emphasized the promotion of DPSC odontogenic differentiation in pulp repair [61, 62]. Unexpectedly, in our study, sensory denervation resulted in an increase in pulpal calcification and enhanced mineralization tendencies of DPSCs, contrary to BMSCs, which showed reduced osteogenic differentiation potential and lead to osteoporosis phenotype in vivo [16]. This phenomenon may be attributed to tissue-specific factors. Additionally, there was no statistically significant difference in DPSC proliferation between the two groups; however, the localization of cell proliferation showed notable distinctions. Reparative dentinogenesis is a complex process requiring DPSC recruitment followed by the signaling of odontoblast-like cell differentiation and dentine secretion [63]. Therefore, the homing of DPSCs to the correct site is a critical factor to be taken into account in pulp repair.

We demonstrated that defects in cell migration play a predominant role in the observed phenotypes after sensory denervation. Such sensory neuron-stem cell crosstalk could be exploited in the treatment of pulp injury, initiating the formation of reparative dentin accurately, consistent with the previous strategy [64]. Efficient chemotaxis results from coordinated chemoattractant gradient sensing, cell polarization, and cellular motility [65]. Prolonged sensory denervation not only loses chemotactic guidance to DPSCs but also alters cell polarity and cellular motility (Fig. 2h, k-n). This phenomenon may be attributed to the CGRP released by sensory nerves, which serves as an endogenous molecule for stem cell maintenance [66]. A low level of CGRP expression is required to preserve the structural and physiological functions of stem cells [67]. Therefore, cell polarity and cellular motility of DPSCs were also changed after pure sensory denervation without pulp injury. However, following pulp injury, CGRP is released in significant quantities, transforming into a chemoattractant with a concentration gradient, which facilitates the recruitment of distant DPSCs. This finding agrees with an experiment in the meniscus that CGRP induces MSCs to enter synovial fluid from the synovium after injury [68]. However, the expression levels of the receptor Ramp1 on DPSCs did not show significant changes following IANX. Consequently, the DPSCs without sensory innervating retain the capacity to restore their migratory capability through the administration of exogenous CGRP, which also provides us with a potential approach to rescue DPSCs with inadequate migration [5].

DPSC migration is not individual cells moving separately, it occurs as a coordinated movement of multiple cells, which is referred to as “collective cell migration”. Collective cell migration is considered a hallmark of tissue remodeling events [69]. Intercellular connections maintain the “supracellular” structure, leading to collective polarization [53]. A group of cells may respond differently in the collective, migrating in a “leader-follower” fashion, when they receive the same chemotactic signals as isolated cells. However, it has been frequently reported in epithelial cells [56]. In our study, DPSCs also exhibit a collective cell migration pattern known as leader-follower migration similar to the migration observed in skin wounds [55]. Even so, this migration pattern is hindered in a nerve-deficient environment. DPSCs in the IANX group showed poorer polarity, looser cell arrangement, and weaker intercellular interactions. Their supracellular structure was disrupted, and collective migration was

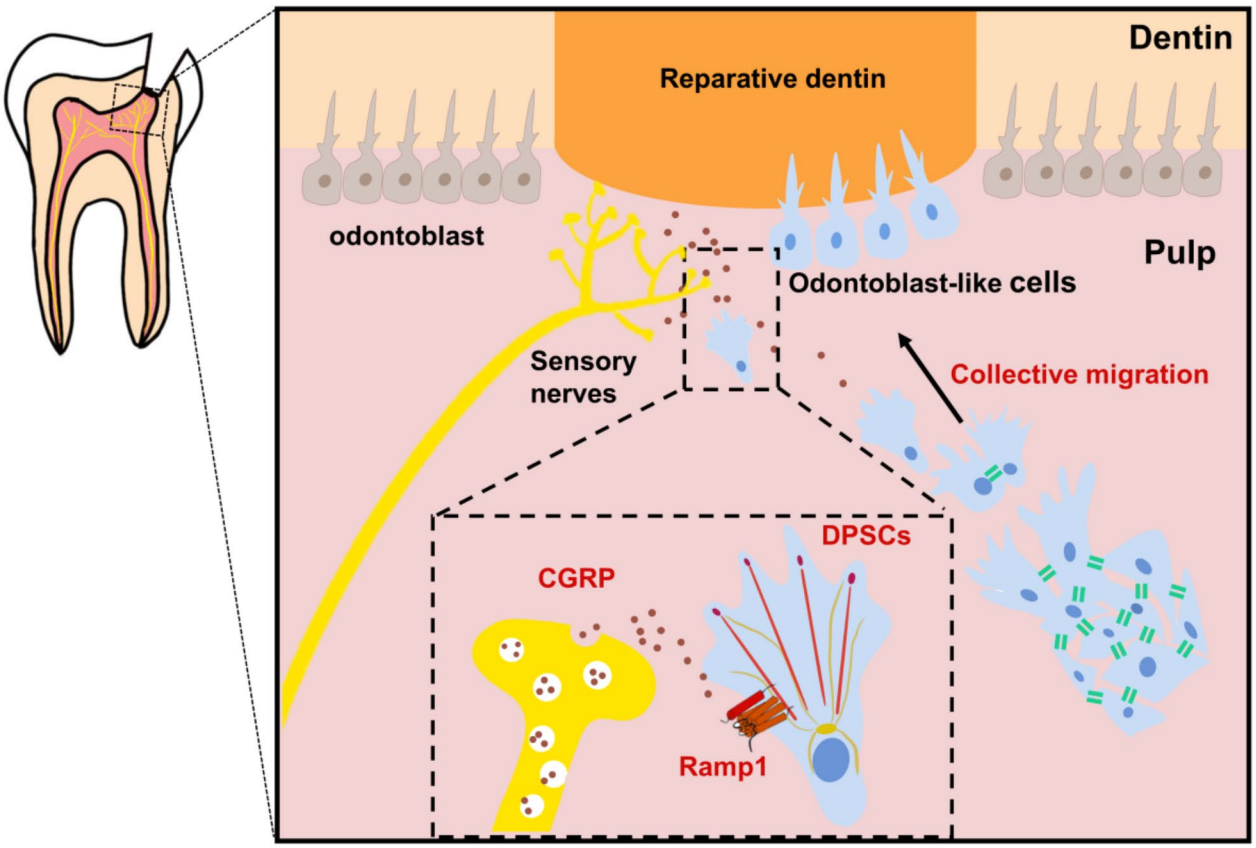

Fig. 7 Sensory nerves foster pulp healing by regulating the collective migration of DPSCs through the CGRP-Ramp1 axis. In the dental pulp, nerve fibers are organized into bundles within the root canal, branching out in the crown pulp, and forming a dense network beneath the odontoblast layer. Sensory nerves are the main constituent of nerves in the dental pulp, which can sense various outer stimuli. After pulp injury, the sensory nerves exhibit a rapid response and sprouting. Concurrently, CGRP is released from sensory nerves near the injury site to act on the receptor Ramp1 on the surface of the activated DPSCs, thereby facilitating the collective cell migration of DPSCs to the injury site by promoting cell polarization and intercellular junctions, thus contributing to the repair of pulp injury

slowed, and also in the LPS injury group (Fig. 5). Nevertheless, after stimulation with CGRP recombinant protein, the intercellular connections and cell polarity of DPSCs were enhanced, and "leader-follower" collective cell migration was accelerated. It is suggested that the release of CGRP from sensory nerves innervating the dental pulp promotes the collective migration of DPSCs after pulp injury, the detailed mechanism underlying this complex and multidimensional phenomenon warrants further research.

Furthermore, the investigation of odontogenic differentiation and proliferation of DPSCs under a sensory-deficient microenvironment, in conjunction with migration, holds academic significance. Interestingly, DPSCs in the IANX group showed reduced N-cadherin expression (Fig. 5c, d), and previous studies have suggested that the knockdown of N-cadherin promoted odontogenic differentiation of DPSCs [70]. However, this is in line with observations of DPSCs in aging pulp, where the nerve density decreases coincidentally. Aging bone density decreases while the aging pulp shows root canal calcification, and it has also been indicated that aging DPSCs have an increased tendency to mineralize [71]. Our findings may explain the increased occurrence of pulp stones and calcification in root canals of elderly individuals, suggesting an advanced involvement of neurodegeneration. Clearly, it is imperative to conduct additional experiments to validate these hypotheses. In terms of proliferation, the DPSC proliferation rate was slowed after IANX, but CGRP did not significantly alter their proliferation rate, consistent with previous in vitro studies [28]. Taken together, we can have increased confidence that sensory nerves promote wound healing mainly by facilitating the migration of DPSCs.

The role of sensory nerves as part of the MSC niche for the maintenance of stem cell homeostasis has gradually come to the forefront in recent years [15, 72]. Regretfully, current studies on the effect of sensory nerves on stem cell

migration are very limited. Exploring and directing the pathways of immature cell transport is essential to elucidate the mechanisms by which stem cells regulate tissue homeostasis and repair [73]. This exploration of stem cell transport mechanisms is beneficial not only to promote endogenous DPSC-mediated pulp repair after injury but also to facilitate the targeted movement of transplanted stem cells from the site of administration to the site of injury [74]. This may provide ideas for the common problem of tunnel defects in dentin bridges and root canal calcification after root capping to modify vital pulp therapy. Together, modulation of sensory nerve release activity could provide a new approach to promote and facilitate the repair of tissue damage, complementing traditional therapies.

Supplementary Information The online version contains supplementary material available at https://doi.org/10.1007/s00018-024-05400-2.

Acknowledgements We thank our lab members for their critical reading of the manuscript and helpful discussions.

Author contributions CMW and QZ contributed to study conception and design. CMW, XCL, JNZ, and ZHZ contributed to data acquisition and analysis. The first draft of the manuscript was written by CMW. XCL and QZ commented on previous versions of the manuscript and critically revised the manuscript. All authors gave final approval and agreed to be accountable for all aspects of the work.

Funding The authors acknowledge the financial support from the National Natural Science Foundation of China (82370950, 82170945).

Data availability The datasets analyzed during the current study are available in the GEO repository. https://www.ncbi.nlm.nih.gov/geo/query/acc.cgi and https://www.ncbi.nlm.nih.gov/geo/query/acc.cgi. Other datasets generated during the current study are not publicly available but are available from the corresponding author on reasonable request.

Declarations

Ethical approval The study was approved by the Ethics Review Board of the Affiliated Stomatology Hospital of Tongji University. All animal experiments were performed in accordance with the International Association for the Study of Pain (IASP) and Federal guidelines protocols approved and ARRIVE guidelines 2.0.

Consent to participate Informed consent was obtained from all individual participants included in the study.

Consent to publish No individual information, image or video was included in this study.

Conflict of interest The authors have no relevant financial or non-financial interests to disclose.

References

1. Kassebaum NJ, Smith AGC, Bernabe E, Fleming TD, Reynolds AE, Vos T, Murray CJL, Marcenes W (2017) Global, Regional, and National Prevalence, incidence, and disability-adjusted life years for oral conditions for 195 countries, 1990–2015: a systematic analysis for the Global Burden of Diseases, injuries, and risk factors. J Dent Res 96(4):380–387. https://doi.org/10.1177/0022034517693566
2. Sui B, Wu D, Xiang L, Fu Y, Kou X, Shi S (2020) Dental Pulp Stem cells: from Discovery to Clinical Application. J Endod 46(9S):S46–S55. https://doi.org/10.1016/j.joen.2020.06.027
3. Duncan HF, Cooper PR, Smith AJ (2019) Dissecting dentine-pulp injury and wound healing responses: consequences for regenerative endodontics. Int Endod J 52(3):261–266. https://doi.org/10.1111/iej.13064
4. Danielyan L, Schwab M, Siegel G, Brawek B, Garaschuk O, Asavapanumas N, Buadze M, Lourhmati A, Wendel HP, Avci-Adali M, Krueger MA, Calaminus C, Naumann U, Winter S, Schaeffeler E, Spogis A, Beer-Hammer S, Neher JJ, Spohn G, Kretschmer A, Kramer-Albers EM, Barth K, Lee HJ, Kim SU, Frey WH 2nd, Claussen CD, Hermann DM, Doeppner TR, Seifried E, Gleiter CH, Northoff H, Schafer R (2020) Cell motility and migration as determinants of stem cell efficacy. EBioMedicine 60:102989. https://doi.org/10.1016/j.ebiom.2020.102989
5. Lampiasi N (2023) The Migration and the fate of Dental Pulp Stem cells. Biology-Basel 12(5). https://doi.org/10.3390/biology12050742
6. Suzuki T, Lee CH, Chen M, Zhao W, Fu SY, Qi JJ, Chotkowski G, Eisig SB, Wong A, Mao JJ (2011) Induced migration of dental pulp stem cells for in vivo pulp regeneration. J Dent Res 90(8):1013–1018. https://doi.org/10.1177/0022034511408426
7. Goichberg P (2016) Current understanding of the pathways involved in adult stem and Progenitor Cell Migration for tissue homeostasis and repair. Stem Cell Rev Rep 12(4):421–437. https://doi.org/10.1007/s12015-016-9663-7
8. Rombouts C, Jeanneau C, Bakopoulou A, About I (2016) Dental Pulp Stem Cell Recruitment Signals within injured Dental Pulp tissue. Dent J (Basel) 4(2):8. https://doi.org/10.3390/dj4020008
9. Picoli CC, Costa AC, Rocha BGS, Silva WN, Santos GSP, Prazeres PHDM, Costa PAC, Oropeza A, da Silva RA, Azevedo VAC, Resende RR, Cunha TM, Mintz A, Birbrair A (2021) Sensory nerves in the spotlight of the stem cell niche. Stem Cells Transl Med 10(3):346–356. https://doi.org/10.1002/sctm.20-0284
10. Peng JY, Chen H, Zhang B (2022) Nerve-stem cell crosstalk in skin regeneration and diseases. Trends Mol Med 28(7):583–595. https://doi.org/10.1016/j.molmed.2022.04.005
11. Machado CV, Passos ST, Campos TMC, Bernardi L, Vilas-Boas DS, Nor JE, Telles PDS, Nascimento IL (2016) The dental pulp stem cell niche based on aldehyde dehydrogenase 1 expression. Int Endod J 49(8):755–763. https://doi.org/10.1111/iej.12511

12. Franca CM, Riggers R, Muschler JL, Widbiller M, Lococo PM, Diogenes A, Bertassoni LE (2019) 3D-Imaging of whole neuronal and vascular networks of the Human Dental Pulp via CLARITY and light sheet Microscopy. Sci Rep 9(1):10860. https://doi.org/10.1038/s41598-019-47221-5
13. Zhan C, Huang M, Yang X, Hou J (2021) Dental nerves: a neglected mediator of pulpitis. Int Endod J 54(1):85–99. https://doi.org/10.1111/iej.13400
14. Gao X, Zhang D, Xu C, Li H, Caron KM, Frenette PS (2021) Nociceptive nerves regulate haematopoietic stem cell mobilization. Nature 589(7843):591–596. https://doi.org/10.1038/s41586-020-03057-y
15. Pei F, Ma L, Jing J, Feng J, Yuan Y, Guo T, Han X, Ho TV, Lei J, He J, Zhang M, Chen JF, Chai Y (2023) Sensory nerve niche regulates mesenchymal stem cell homeostasis via FGF/mTOR/autophagy axis. Nat Commun 14(1):344. https://doi.org/10.1038/s41467-023-35977-4
16. Jones RE, Salhotra A, Robertson KS, Ransom RC, Foster DS, Shah HN, Quarto N, Wan DC, Longaker MT (2019) Skeletal stem cell-Schwann Cell Circuitry in Mandibular Repair. Cell Rep 28(11):2757–2766e5. https://doi.org/10.1016/j.celrep.2019.08.021
17. Naji A, Eitoku M, Favier B, Deschaseaux F, Rouas-Freiss N, Suganuma N (2019) Biological functions of mesenchymal stem cells and clinical implications. Cell Mol Life Sci 76(17):3323–3348. https://doi.org/10.1007/s00018-019-03125-1
18. Fu XR, Liu G, Halim A, Ju Y, Luo Q, Song GB (2019) Mesenchymal stem cell Migration and tissue repair. Cells 8(8). https://doi.org/10.3390/cells8080784
19. Eseonu OI, De Bari C (2015) Homing of mesenchymal stem cells: mechanistic or stochastic? Implications for targeted delivery in arthritis. Rheumatology 54(2):210–218. https://doi.org/10.1093/rheumatology/keu377
20. Pinho-Ribeiro FA, Verri WA Jr., Chiu IM (2017) Nociceptor sensory Neuron-Immune interactions in Pain and inflammation. Trends Immunol 38(1):5–19. https://doi.org/10.1016/j.it.2016.10.001
21. Tao RY, Mi BB, Hu YQ, Lin S, Xiong Y, Lu X, Panayi AC, Li G, Liu GH (2023) Hallmarks of peripheral nerve function in bone regeneration. Bone Res 11(1). https://doi.org/10.1038/s41413-022-00240-x
22. Wan QQ, Qin WP, Ma YX, Shen MJ, Li J, Zhang ZB, Chen JH, Tay FR, Niu LN, Jiao K (2021) Crosstalk between bone and nerves within bone. Adv Sci (Weinh) 8(7):2003390. https://doi.org/10.1002/advs.202003390
23. Jia S, Zhang SJ, Wang XD, Yang ZH, Sun YN, Gupta A, Hou R, Lei DL, Hu KJ, Ye WM, Wang L (2019) Calcitonin gene-related peptide enhances osteogenic differentiation and recruitment of bone marrow mesenchymal stem cells in rats. Exp Ther Med 18(2):1039–1046. https://doi.org/10.3892/etm.2019.7659
24. Nam D, Park A, Dubon MJ, Yu J, Kim W, Son Y, Park KS (2020) Coordinated regulation of Mesenchymal Stem Cell Migration by various chemotactic stimuli. Int J Mol Sci 21(22). https://doi.org/10.3390/ijms21228561
25. Wang Y, Zhang D, Ashraf M, Zhao T, Huang W, Ashraf A, Balasubramaniam A (2010) Combining neuropeptide Y and mesenchymal stem cells reverses remodeling after myocardial infarction. Am J Physiol Heart Circ Physiol 298(1):H275–H286. https://doi.org/10.1152/ajpheart.00765.2009
26. Moore ER, Michot B, Erdogan O, Ba A, Gibbs JL, Yang Y (2022) CGRP and shh mediate the Dental Pulp Cell response to Neuron Stimulation. J Dent Res 101(9):1119–1126. https://doi.org/10.1177/00220345221086858
27. Wei XL, Luo L, Chen MZ, Zhou J, Lan BY, Ma XM, Chen WX (2023) Temporospatial expression of Neuropeptide Substance P in Dental Pulp Stem cells during Odontoblastic differentiation in Vitro and reparative dentinogenesis in vivo. J Endod 49(3):276–285. https://doi.org/10.1016/j.joen.2022.12.006
28. Michot B, Casey SM, Gibbs JL (2020) Effects of Calcitonin Gene-related peptide on Dental Pulp Stem Cell viability, proliferation, and differentiation. J Endod 46(7):950–956. https://doi.org/10.1016/j.joen.2020.03.010
29. Fujiwara S, Urata K, Oto T, Hayashi Y, Hitomi S, Iwata K, Iinuma T, Shinoda M (2023) Age-related changes in trigeminal ganglion macrophages enhance Orofacial Ectopic Pain after Inferior Alveolar nerve Injury. Vivo 37(1):132–142. https://doi.org/10.21873/invivo.13062
30. Hayano S, Fukui Y, Kawanabe N, Kono K, Nakamura M, Ishihara Y, Kamioka H (2018) Role of the inferior alveolar nerve in Rodent Lower Incisor Stem cells. J Dent Res 97(8):954–961. https://doi.org/10.1177/0022034518758244
31. Liu AQ, Zhang LS, Fei DD, Guo H, Wu ML, Liu J, He XN, Zhang YJ, Xuan K, Li B (2020) Sensory nerve-deficient microenvironment impairs tooth homeostasis by inducing apoptosis of dental pulp stem cells. Cell Prolif 53(5). https://doi.org/10.1111/cpr.12803
32. Matsumura S, Quispe-Salcedo A, Schiller CM, Shin JS, Locke BM, Yakar S, Shimizu E (2017) IGF-1 mediates EphrinB1 activation in regulating Tertiary dentin formation. J Dent Res 96(10):1153–1161. https://doi.org/10.1177/0022034517708572
33. Chen J, Xu HX, Xia K, Cheng SH, Zhang Q (2021) Resolvin E1 accelerates pulp repair by regulating inflammation and stimulating dentin regeneration in dental pulp stem cells. Stem Cell Res Ther 12(1). https://doi.org/10.1186/s13287-021-02141-y
34. Liu XC, Wang CM, Pang LP, Pan LL, Zhang Q (2022) Combination of resolvin E1 and lipoxin A4 promotes the resolution of pulpitis by inhibiting NF-kappa B activation through upregulating sirtuin 7 in dental pulp fibroblasts. Cell Prolif 55(5). https://doi.org/10.1111/cpr.13227
35. Austah ON, Lillis KV, Akopian AN, Harris SE, Grinceviciute R, Diogenes A (2022) Trigeminal neurons control immune-bone cell interaction and metabolism in apical periodontitis. Cell Mol Life Sci 79(6). https://doi.org/10.1007/s00018-022-04335-w
36. Liu L, Dana R, Yin J (2020) Sensory neurons directly promote angiogenesis in response to inflammation via substance P signaling. FASEB J 34(5):6229–6243. https://doi.org/10.1096/fj.201903236R
37. Couve E, Lovera M, Suzuki K, Schmachtenberg O (2018) Schwann Cell phenotype changes in Aging Human Dental Pulp. J Dent Res 97(3):347–355. https://doi.org/10.1177/0022034517733967
38. Contreras C, Cádiz B, Schmachtenberg O (2023) Determination of the severity of Pulpitis by Immunohistological Analysis and Comparison with the clinical picture. J Endod 49(1):26–35. https://doi.org/10.1016/j.joen.2022.10.012
39. Guo YS, Chi XP, Wang YF, Heng BC, Wei Y, Zhang XH, Zhao H, Yin Y, Deng XL (2020) Mitochondria transfer enhances proliferation, migration, and osteogenic differentiation of bone marrow mesenchymal stem cell and promotes bone defect healing. Stem Cell Res Ther 11(1). https://doi.org/10.1186/s13287-020-01704-9
40. Kim DS, Lee JK, Kim JH, Lee J, Kim DS, An S, Park SB, Kim TH, Rim JS, Lee S, Han DK (2021) Advanced PLGA hybrid scaffold with a bioactive PDRN/BMP2 nanocomplex for angiogenesis and bone regeneration using human fetal MSCs. Sci Adv 7(50). https://doi.org/10.1126/sciadv.abj1083
41. Watanabe M, Okamoto M, Komichi S, Huang H, Matsumoto S, Moriyama K, Ohshima J, Abe S, Morita M, Ali M, Takebe K, Kozaki I, Fujimoto A, Kanie K, Kato R, Uto K, Ebara M, Yamawaki-Ogata A, Narita Y, Takahashi Y, Hayashi M (2023) Novel functional peptide for Next-Generation Vital Pulp Therapy. J Dent Res 102(3):322–330. https://doi.org/10.1177/00220345221135766

42. Chen SQ, Chen XY, Cui YZ, Yan BX, Zhou Y, Wang ZY, Xu F, Huang YZ, Zheng YX, Man XY (2022) Cutaneous nerve fibers participate in the progression of psoriasis by linking epidermal keratinocytes and immunocytes. Cell Mol Life Sci 79(5):267. https://doi.org/10.1007/s00018-022-04299-x
43. Couve E, Osorio R, Schmachtenberg O (2014) Reactionary dentinogenesis and Neuroimmune Response in Dental Caries. J Dent Res 93(8):788–793. https://doi.org/10.1177/0022034514539507
44. Couve E, Schmachtenberg O (2018) Schwann cell responses and plasticity in different Dental pulp scenarios. Front Cell Neurosci 12. https://doi.org/10.3389/fncel.2018.00299
45. Li Z, Meyers CA, Chang L, Lee S, Li Z, Tomlinson R, Hoke A, Clemens TL, James AW (2019) Fracture repair requires TrkA signaling by skeletal sensory nerves. J Clin Invest 129(12):5137–5150. https://doi.org/10.1172/JCI128428
46. Kok ZY, Alaidaroos NYA, Alraies A, Colombo JS, Davies LC, Waddington RJ, Sloan AJ, Moseley R (2022) Dental Pulp Stem Cell Heterogeneity: finding Superior Quality needles in a Dental Pulpal Haystack for Regenerative Medicine-based applications. Stem Cells Int 2022. https://doi.org/10.1155/2022/9127074
47. Esteves CL, Sheldrake TA, Dawson L, Menghini T, Rink BE, Amilon K, Khan N, Peault B, Donadeu FX (2017) Equine mesenchymal stromal cells retain a Pericyte-Like phenotype. Stem Cells Dev 26(13):964–972. https://doi.org/10.1089/scd.2017.0017
48. Dahlhaus M, Roos J, Engel D, Tews D, Halbgebauer D, Funcke JB, Kiener S, Schuler PJ, Doscher J, Hoffmann TK, Zinngrebe J, Rojewski M, Schrezenmeier H, Debatin KM, Wabitsch M, Fischer-Posovszky P (2020) CD90 is dispensable for White and Beige/Brown Adipocyte differentiation. Int J Mol Sci 21(21). https://doi.org/10.3390/ijms21217907
49. Widbiller M, Eidt A, Wolflick M, Lindner SR, Schweikl H, Hiller KA, Buchalla W, Galler KM (2018) Interactive effects of LPS and dentine matrix proteins on human dental pulp stem cells. Int Endod J 51(8):877–888. https://doi.org/10.1111/iej.12897
50. Flegel C, Schobel N, Altmuller J, Becker C, Tannapfel A, Hatt H, Gisselmann G (2015) RNA-Seq analysis of human trigeminal and dorsal Root Ganglia with a focus on chemoreceptors. PLoS ONE 10(6):e0128951. https://doi.org/10.1371/journal.pone.0128951
51. Huang S, Ziegler CGK, Austin J, Mannoun N, Vukovic M, Ordovas-Montanes J, Shalek AK, von Andrian UH (2021) Lymph nodes are innervated by a unique population of sensory neurons with immunomodulatory potential. Cell 184(2):441–459e25. https://doi.org/10.1016/j.cell.2020.11.028
52. Pinho-Ribeiro FA, Deng LW, Neel DV, Erdogan O, Basu H, Yang DP, Choi S, Walker AJ, Carneiro-Nascimento S, He KT, Wu GD, Stevens B, Doran KS, Levy D, Chiu IM (2023) Bacteria hijack a meningeal neuroimmune axis to facilitate brain invasion. Nature. https://doi.org/10.1038/s41586-023-05753-x
53. Mayor R, Etienne-Manneville S (2016) The front and rear of collective cell migration. Nat Rev Mol Cell Biol 17(2):97–109. https://doi.org/10.1038/nrm.2015.14
54. Etienne-Manneville S (2004) Cdc42–the centre of polarity. J Cell Sci 117(Pt 8):1291–1300. https://doi.org/10.1242/jcs.01115
55. Jiang D, Christ S, Correa-Gallegos D, Ramesh P, Kalgudde Gopal S, Wannemacher J, Mayr CH, Lupperger V, Yu Q, Ye H, Muck-Hausl M, Rajendran V, Wan L, Liu J, Mirastschijski U, Volz T, Marr C, Schiller HB, Rinkevich Y (2020) Injury triggers fascia fibroblast collective cell migration to drive scar formation through N-cadherin. Nat Commun 11(1):5653. https://doi.org/10.1038/s41467-020-19425-1
56. Kozyrska K, Pilia G, Vishwakarma M, Wagstaff L, Goschorska M, Cirillo S, Mohamad S, Gallacher K, Carazo Salas RE, Piddini E (2022) p53 directs leader cell behavior, migration, and clearance during epithelial repair. Science 375(6581):eabl8876. https://doi.org/10.1126/science.abl8876
57. Zhang W, Lyu M, Bessman NJ, Xie Z, Arifuzzaman M, Yano H, Parkhurst CN, Chu C, Zhou L, Putzel GG, Li T-T, Jin W-B, Zhou J, Hu H, Tsou AM, Guo C-J, Artis D (2022) Gut-innervating nociceptors regulate the intestinal microbiota to promote tissue protection. Cell 185(22):4170–4189e20. https://doi.org/10.1016/j.cell.2022.09.008
58. Yang D, Jacobson A, Meerschaert KA, Sifakis JJ, Wu M, Chen X, Yang T, Zhou Y, Anekal PV, Rucker RA, Sharma D, Sontheimer-Phelps A, Wu GS, Deng L, Anderson MD, Choi S, Neel D, Lee N, Kasper DL, Jabri B, Huh JR, Johansson M, Thiagarajah JR, Riesenfeld SJ, Chiu IM (2022) Nociceptor neurons direct goblet cells via a CGRP-RAMP1 axis to drive mucus production and gut barrier protection. Cell 185(22):4190–4205e25. https://doi.org/10.1016/j.cell.2022.09.024
59. Naftel JP, Richards LP, Pan M, Bernanke JM (1999) Course and composition of the nerves that supply the mandibular teeth of the rat. Anat Rec 256(4):433–447. https://doi.org/10.1002/(Sici)1097-0185(19991201)256:4 <433::Aid-Ar10>3.0.Co;2-R
60. Dammaschke T (2010) Rat molar teeth as a study model for direct pulp capping research in dentistry. Lab Anim 44(1):1–6. https://doi.org/10.1258/la.2009.008120
61. Wang S, Gao X, Gong W, Zhang Z, Chen X, Dong Y (2014) Odontogenic differentiation and dentin formation of dental pulp cells under nanobioactive glass induction. Acta Biomater 10(6):2792–2803. https://doi.org/10.1016/j.actbio.2014.02.013
62. Huang M, Hill RG, Rawlinson SC (2016) Strontium (Sr) elicits odontogenic differentiation of human dental pulp stem cells (hDPSCs): a therapeutic role for Sr in dentine repair? Acta Biomater 38:201–211. https://doi.org/10.1016/j.actbio.2016.04.037
63. da Rosa WLO, Piva E, da Silva AF (2018) Disclosing the physiology of pulp tissue for vital pulp therapy. Int Endod J 51(8):829–846. https://doi.org/10.1111/iej.12906
64. Zhang J, Zhu LX, Cheng X, Lin Y, Yan P, Peng B (2015) Promotion of Dental Pulp Cell Migration and Pulp Repair by a Bioceramic Putty Involving FGFR-mediated signaling pathways. J Dent Res 94(6):853–862. https://doi.org/10.1177/0022034515572020
65. Aase K, Ernkvist M, Ebarasi L, Jakobsson L, Majumdar A, Yi C, Birot O, Ming Y, Kvanta A, Edholm D, Aspenstrom P, Kissil J, Claesson-Welsh L, Shimono A, Holmgren L (2007) Angiomotin regulates endothelial cell migration during embryonic angiogenesis. Genes Dev 21(16):2055–2068. https://doi.org/10.1101/gad.432007
66. Lv XT, Chen QQ, Zhang SY, Gao F, Liu QC (2022) CGRP: a new endogenous cell stemness maintenance molecule. Oxid Med Cell Longev 2022:4107433. https://doi.org/10.1155/2022/4107433
67. Xie WL, Fisher JT, Lynch TJ, Luo MH, Evans TIA, Neff TL, Zhou WH, Zhang L, Ou Y, Bunnett NW, Russo AF, Goodheart MJ, Parekh KR, Liu XM, Engelhardt JF (2011) CGRP induction in cystic fibrosis airways alters the submucosal gland progenitor cell niche in mice. J Clin Invest 121(8):3144–3158. https://doi.org/10.1172/Jci41857
68. Watanabe N, Endo K, Komori K, Ozeki N, Mizuno M, Katano H, Kohno Y, Tsuji K, Koga H, Sekiya I (2020) Mesenchymal stem cells in synovial fluid increase in Knees with degenerative Meniscus Injury after arthroscopic procedures through the endogenous effects of CGRP and HGF. Stem Cell Rev Rep 16(6):1305–1315. https://doi.org/10.1007/s12015-020-10047-0
69. Friedl P, Gilmour D (2009) Collective cell migration in morphogenesis, regeneration and cancer. Nat Rev Mol Cell Biol 10(7):445–457. https://doi.org/10.1038/nrm2720
70. Deng Z, Yan W, Dai X, Chen M, Qu Q, Wu B, Zhao W (2021) N-Cadherin regulates the odontogenic differentiation of Dental Pulp Stem cells via beta-catenin activity. Front Cell Dev Biol 9:661116. https://doi.org/10.3389/fcell.2021.661116

71. Morsczeck C (2019) Cellular senescence in dental pulp stem cells. Arch Oral Biol 99:150–155. https://doi.org/10.1016/j.archoralbio.2019.01.012
72. Picoli CC, Costa AC, Rocha BGS, Silva WN, Santos GSP, Prazeres P, Costa PAC, Oropeza A, da Silva RA, Azevedo VAC, Resende RR, Cunha TM, Mintz A, Birbrair A (2021) Sensory nerves in the spotlight of the stem cell niche. Stem Cells Transl Med 10(3):346–356. https://doi.org/10.1002/sctm.20-0284
73. de Lucas B, Perez LM, Galvez BG (2018) Importance and regulation of adult stem cell migration. J Cell Mol Med 22(2):746–754. https://doi.org/10.1111/jcmm.13422
74. Yin Y, Li X, He XT, Wu RX, Sun HH, Chen FM (2017) Leveraging stem cell homing for therapeutic regeneration. J Dent Res 96(6):601–609. https://doi.org/10.1177/0022034517706070